Stereoselective Excited-State Isomerization and Decay Paths in cis-Cyclobiazobenzene

Teng-Shuo Zhang, Zi-Wen Li, Qiu Fang, Mario Barbatti, Wei-Hai Fang, Ganglong Cui

Stereoselective Excited-State Isomerization and Decay Paths in cis-Cyclobiazobenzene

Teng-Shuo Zhang[1], Zi-Wen Li[1], Qiu Fang[1], Mario Barbatti[2*], Wei-Hai Fang, and Ganglong Cui[1]*

[1]*Key Laboratory of Theoretical and Computational Photochemistry, Ministry of Education, College of Chemistry, Beijing Normal University, Beijing 100875, P. R. China*

[2]*Aix Marseille Univ, CNRS, ICR, Marseille, France*

E-mail: ganglong.cui@bnu.edu.cn and mario.barbatti@univ-amu.fr

Abstract

Herein we have employed OM2/MRCI-based full-dimensional nonadiabatic dynamics simulations to explore the photoisomerization and subsequent excited-state decay of a macrocyclic cyclobiazobenzene (CBA) molecule. Two S_1/S_0 conical intersection structures are found to be responsible for the excited-state decay. Related to these two conical intersections, we found two stereoselective photoisomerization and excited-state decay pathways, which correspond to the clockwise and counterclockwise rotation motions with respect to the N=N bond of the azo group. In both pathways the excited-state isomerization is ultrafast and finishes within ca. 69 fs; but, the clockwise isomerization channel is much more favorable than the counterclockwise one with a ratio of 74% vs. 26%. Importantly, the present work demonstrates that stereoselective pathways exist not only in the photoisomerization of isolated azobenzene-like systems but also in macrocyclic systems with multiple azobenzenes (ABs). This finding could provide useful insights for understanding and controlling the photodynamics of macrocyclic nanostructures with AB units as the main building units.

INTRODUCTION

Azobenzene (AB), as one of the most studied photoswitchable compounds, has various potential applications ranging from photopharmacology via optochemical genetics to data storage because it is easily synthesized experimentally and highly stable, and presents high extinction coefficients and isomerization quantum yields.[1–4] Owing to its importance, in the past decade, many AB derivatives have been synthesized and applied in optical switches, reversible nanostructures, molecular machines, etc.[5–14] To get in-depth atomistic insights, computational studies have also been carried out, in companying with experimental studies, to explore photoinduced isomerization reactions and related dynamics of AB and its variants in the gas phase, in various solutions, and linked to peptides and nucleic acids.[15–43] Nevertheless, most of previous experimental and computational studies are mainly focused on isolated AB and linearly linked ABs in complex surroundings.[44-47]

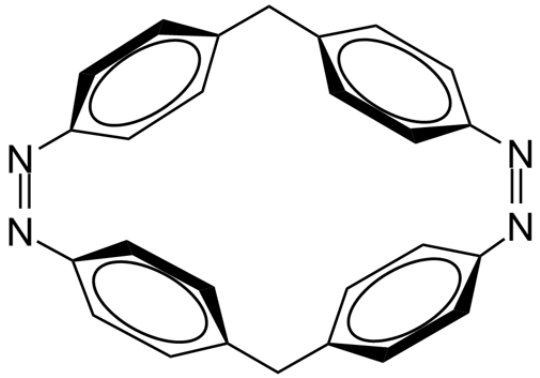

Figure 1. Our studied cyclobiazobenzene molecule in which two azobenzene units are linked by the covalent bonds.

In recent years, photoswitchable macrocyclic systems with multiple ABs have been explored experimentally because of their potential applications in supramolecular chemistry, molecular machines, etc.[6,48-51] These AB units are usually linked by chemical bonds, which thus leads to

remarkable steric interaction and ring strain. Very recently, Slavov et al. have employed time-resolved absorption spectroscopy to explore the excited-state dynamics of a macrocyclic biazobenzene molecule (CBA) as shown in Figure 1.[52] They found that upon continuous excitation on the most stable (Z,Z) isomer of CBA, it does not generate either (Z,E) or (E,E) isomers. This is ascribed to a very fast thermal back-isomerization of the (Z,E) isomer induced by large ring strain that is caused by the ultrafast excited-state photoisomerization process. This fast back reaction prevents the accumulation of both (Z,E) and (E,E) isomers. They have found that the individual AB unit still undergoes an ultrafast cis-trans photoisomerization in spite of the existence of strong steric hindrance. This interaction also breaks the molecular symmetry and finally gives rise to an enhanced adsorption intensity for the weak $^1n\pi^*$ singlet state. The experiments also indicate that both $^1n\pi^*$ and $^1\pi\pi^*$ singlet states of the (Z,Z) isomer of CBA have similar kinetics, and the main photoisomerization is completed within about 200 fs, followed by a ground-state cooling process. Although TD-DFT calculations have qualitatively rationalized some experimental phenomena, the photoisomerization and excited-state decay dynamics of this CBA molecule is far from a complete understanding, and it has not been explored by full-dimensional nonadiabatic dynamics simulations until now. In this work, we fill this knowledge gap and aim at exploring the CBA photoisomerization dynamics starting from its (Z,Z) conformer upon excitation to its weak $^1n\pi^*$ singlet state. Based on our "on-the-fly" dynamic simulations, we have identified the excited-state photoisomerization and excited-state decay mechanism. Moreover, our results reveal, for the first time, two stereoselective excited-state decay pathways in this macrocyclic CBA system.

COMPUTATIONAL DETAILS

Ground-state conformers of CBA are first optimized using the density functional theory (DFT) method1 with the globally hybrid B3LYP exchange-correlation functional.[53-57] The 6-31G* basis

set is employed for all DFT computations,[58,59] which are carried out using GAUSSIAN09.[53,60,61] Minima, conical intersections, and minimum-energy potential energy profiles in the S_0 and S_1 singlet states are optimized using the OM2/MRCI method, which has been extensively demonstrated to be very accurate for the description of the excited states of azobenzene and its variants. [32,35,40,62-64]

All semi-empirical calculations were performed using the MNDO99 code.[65-68] During geometry optimizations and dynamics simulations, all required energies, gradients, and nonadiabatic coupling elements were computed analytically. Minimum-energy conical intersections were optimized using the Lagrange-Newton approach.[69,70] In the OM2/MRCI calculations, the restricted open-shell HF formalism is applied in the self-consistent field (SCF) treatment. The active space in the MRCI calculations includes 8 electrons in 6 orbitals (see Figure S1). In terms of the SCF configuration, it comprises the 4 highest doubly-occupied orbitals and the 2 lowest unoccupied orbitals. For the MRCI treatment, three configuration state functions are chosen as references, namely the SCF configuration and the two closed-shell configurations derived therefrom (i.e., all singlet configurations that can be generated from HOMO and LUMO of the closed-shell ground state). The MRCI wavefunction is built by allowing all single and double excitations from these three references.

The S_1 nonadiabatic dynamics simulations are studied by performing 300 fs OM2/MRCI trajectory surface-hopping simulations.[71-83] The initial atomic coordinates and velocities for the S_1 photodynamics simulations are randomly selected from a 10 ps canonical molecular dynamics trajectory in the ground state. The numbers of excited-state dynamics runs are then chosen according to the computed S_0-S_1 transition probabilities. A total of 425 surface-hopping trajectories are run for the S_1 photodynamics, with all relevant energies, gradients, and

nonadiabatic coupling vectors being computed on-the-fly as needed. For points with an energy gap of less than 10 kcal/mol, the fewest-switches criterion is applied to decide whether to hop. The time step is chosen to be 0.1 fs for the nuclear motion and 0.0005 fs for the electronic propagation. The unitary propagator evaluated at mid-point is used to propagate the electronic motion. The translational and rotational motions are removed in each step. The empirical decoherence correction (0.1 au) by Granucci et al. is employed.[84] The final evaluations are done for 417 trajectories that finish successfully in the photodynamics and that satisfies our energy continuity criterion and total energy conservation criterion (absolute energy difference less than 2 kcal/mol in 99.794% of time steps; see Figure S2-S4). The adapted time step by Thiel et al. will be used to treat the energy continuity issue in the future.[85] Further technical details are given in previous publications.[86-95]

RESULTS AND DISCUSSION

In the S_0 state, there are three main stable structures with respect to the trans and cis conformations of the two azo groups, which are referred to as S0-ZZ, S0-ZE, and S0-EE. Since we are mainly focused on exploring the photoinduced excited-state relaxation dynamics from the most stable S0-ZZ structure, only S0-ZZ and S0-ZE structures are heavily relevant and, therefore, optimized at the OM2/MRCI level, as shown in Figure 2. In S0-ZZ, both N3-N4 and N3'-N4' bond lengths are calculated to be 1.191 and 1.191 Å and the C2N3N4C5 and C2'N3'N4'C5' dihedral angles are 2.6° and 2.6° at the OM2/MRCI level, respectively. In S0-ZE, the bond length of the N3-N4 bond that is still in the cis conformation is estimated to be 1.192 Å; while, that of the N3'-N4' bond, which has already isomerized into the trans conformation, is increased to 1.214 Å. Remarkably, the C2N3N4C5 and C2'N3'N4'C5' dihedral angles are estimated to be 5.6° and

143.6°, respectively. The strong strain interaction makes these dihedral angles deviate from their typical values, 0° in the cis conformation and 180° in the trans one, observed in AB variants without external strain effects.

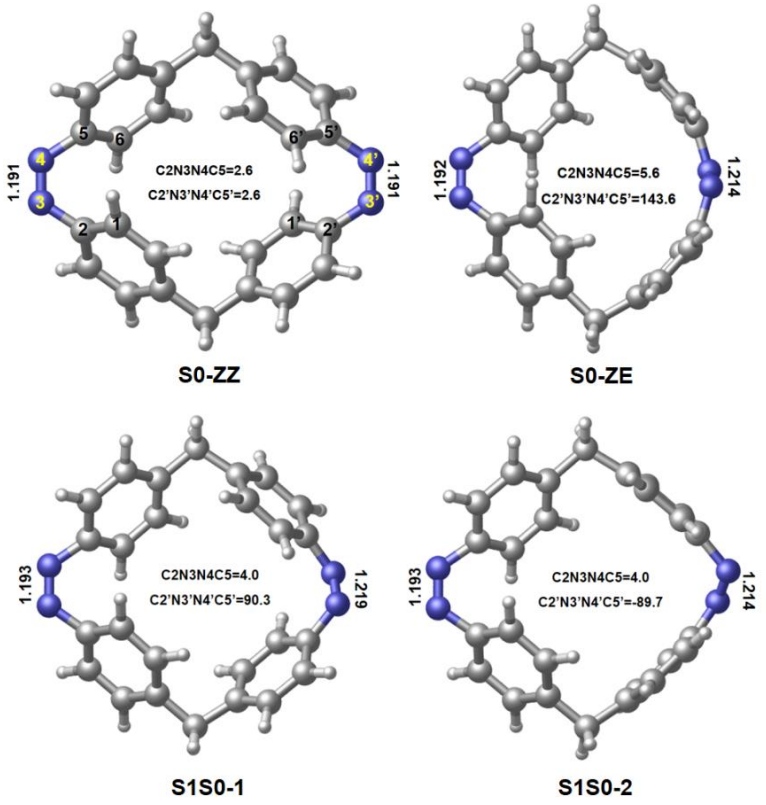

Figure 2. (Top panel) Stable (Z, Z) and (Z, E) conformers referred to as S0-ZZ and S0-ZE; (bottom panel) minimum-energy S_1/S_0 conical intersections referred to as S1S0-1 and S1S0-2. Also shown are selected geometric parameters optimized at the OM2/MRCI level.

At the Franck-Condon region, the first excited singlet state is of $^1n\pi^*$ character and is mainly composed of the HOMO-LUMO electronic configuration. The vertical excitation energy is 75.0 kcal/mol and the corresponding oscillator strength is 0.10 at the OM2/MRCI level. Compared with that of isolated AB molecule, the oscillator strength of the $^1n\pi^*$ singlet state in CBA is comparably enhanced, which is consistent with recent experimental observation.[52]

Two S_1/S_0 minimum-energy conical intersections (MECIs) relevant to the cis-trans photoisomerization of the N3'-N4' azo group of CBA are optimized at the OM2/MRCI level and are referred to as S1S0-1 and S1S0-2 in Figure 2. These two MECI structures are all related to the N3'-N4' azo group; however, they have different C2'N3'N4'C5' dihedral angles, which are 90.3° in S1S0-1 and -89.7° in S1S0-2. At the OM2/MRCI level, both of them have similar potential energies, 54.6 and 56.3 kcal/mol. Nevertheless, their dynamical roles in the excited-state relaxation dynamics are different (see below).

To gain insights into time-dependent excited-state properties, e.g., the S_1 lifetime, the excited-state deactivation channels, and the interplay of the competitive excited-state channels, we have performed hundreds of nonadiabatic surface-hopping dynamics runs (417 successful trajectories out 425 ones). Our simulations are carried out at the semi-empirical OM2/MRCI level, which has been demonstrated accurate enough to simulate the topological structures of the S_0 and S_1 potential energy surfaces of AB variants in many previous studies.[32,35,40,62-64] In our simulations the S_1 state is chosen as the initially populated excited singlet state.

The left panel of Figure 3 shows the distribution of the two dihedral angles relevant to the cis-trans photoisomerization at all the $S_1 \rightarrow S_0$ hopping points as well as at the initial Franck-Condon region. All trajectories start from the S0-ZZ Franck-Condon region, where both C2N3N4C5 and C2'N3'N4'C5' dihedral angles are around 0°. Interestingly, one can see that there are four hopping regions (in red and blue in the left panel of Figure 3). It should be noted that the photoisomerization channel related to the N3N4 azo group is essentially the same as that related to the N3'N4' azo group due to the molecular symmetry, so these four hopping patterns actually correspond to two different hopping channels, which are separately related to the two S_1/S_0 conical intersection regions, namely S1S0-1 and S1S0-2 discussed above.

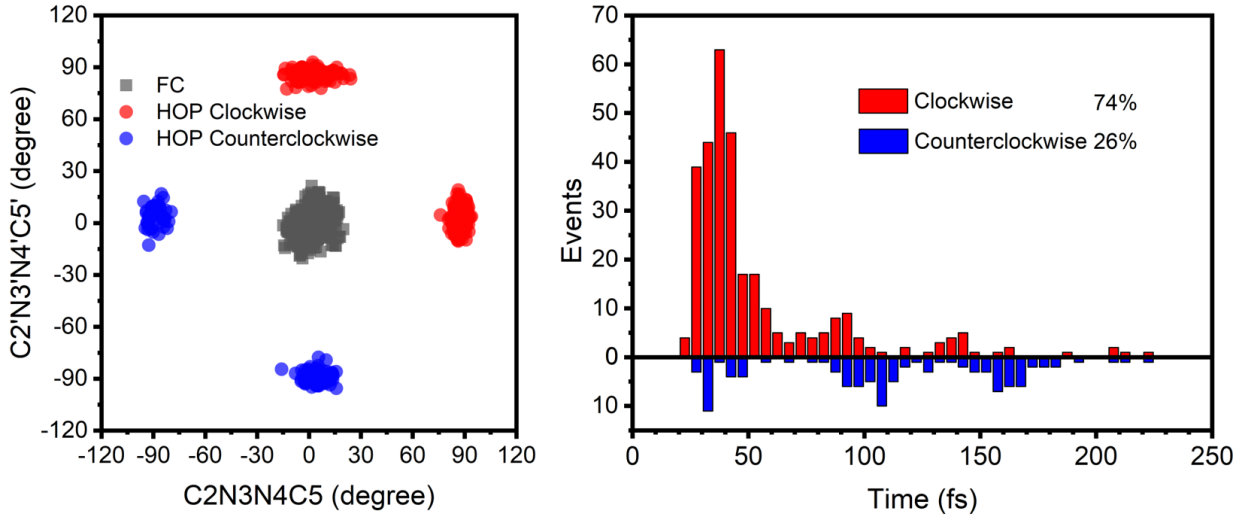

Figure 3. Distributions of (left) the selected geometric parameters at the $S_1 \rightarrow S_0$ hopping points and (right) the corresponding hopping times. See text for discussion.

It is a clockwise motion from S0-ZZ to S1S0-1 because the C2'N3'N4'C5' dihedral angle changes from 8.6° in S0-ZZ to 90.3° to S1S0-1; whereas, it is a counterclockwise from S0-ZZ to S1S0-2 because this dihedral angle changes from 8.6° in S0-ZZ to -89.7° to S1S0-2. It is natural to ask which channel plays a more important role in the excited-state relaxation process. This question is answered by the right panel of Figure 3, from which one can find that the clockwise excited-state deactivation channel via S1S0-1 is more favorable than that via S1S0-2, by 74% vs. 26% in terms of our nonadiabatic dynamics simulations. This ratio is close to that observed in AB molecule but smaller than our recently studied azobenzene-like molecule.[96] It should be also noted that the photoinduced unidirectional motion has been observed in many recent works.[97-100]

To understand why the first channel via S1S0-1 is preferred dynamically, the S_1 minimum-energy relaxation paths from S0-ZZ to either S1S0-1 or S1S0-2 are calculated at the OM2/MRCI level. As shown in Figure 4, it is apparent that the path from S0-ZZ to S1S0-2 has a small barrier

of 3.7 kcal/mol in the S_1 state; while, it is barrierless from S0-ZZ to S1S0-1. This explains the trends about the preference of the $S_1 \rightarrow S_0$ hopping regions observed in our dynamical results.

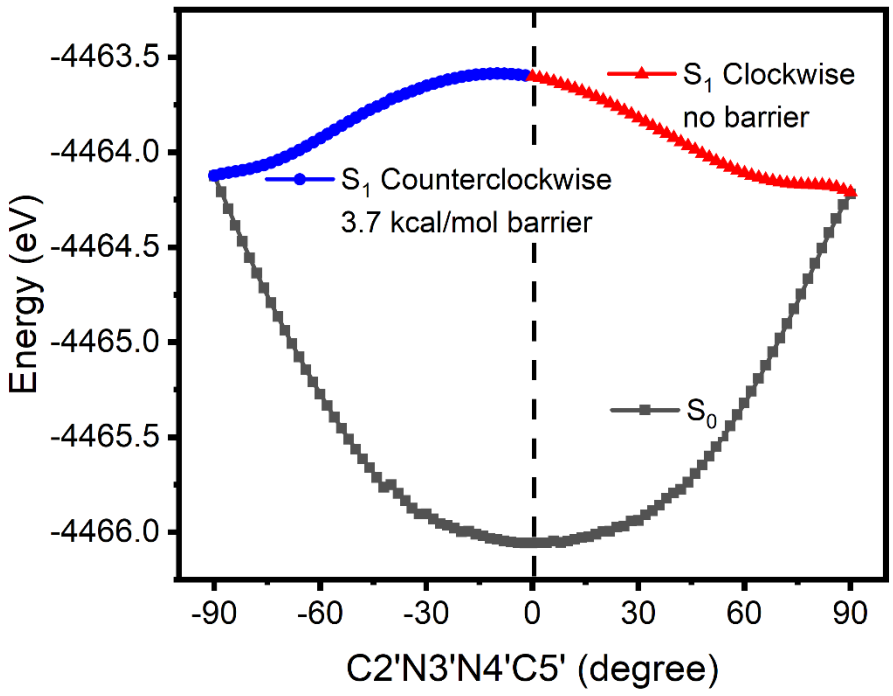

Figure 4. OM2/MRCI optimized (S_1) minimum-energy paths along the clockwise (red) and counterclockwise (blue) isomerization directions.

Figure S5 shows the time-dependent state populations of both S_1 and S_0 states on the basis of the nonadiabatic trajectories. It is clear that in the first 25 fs, there is no excited-state hopping occurring. This period corresponds to the S_1 excited-state relaxation from the Franck-Condon to conical intersection regions. After that, the hopping takes place and the S_1 state population starts to decrease gradually to zero at the end of 300 fs simulation time. Of course, in the same time, the S_0 state population increases accordingly. Through fitting the S_1 state population via a simple exponential function of $y = exp(-(t - t_0) / k)$ in which $t_0 = 22$ fs, the S_1 excited-state lifetime i.e. $t_0 + k$ is estimated to be 69 fs, which is close to those of previously studied AB derivatives.[16,32,33,36]

The distribution of final products at the end of 300 fs simulation time is shown in Figure S6. It is clear that there are three main product regions: 41% of trajectories stay in the region near S0-ZZ; 43% stop in the region near S0-ZE with the clockwise C2'N3'N4'C5' dihedral angle; and 16% are in the region near S0-ZE with the counterclockwise C2'N3'N4'C5' dihedral angle. This final product yield is consistent with our electronic structure calculations. As discussed above, for S0-ZZ, only one conformer exists as demonstrated in Figure 4; but, for S0-ZE, there are two isoenergetic conformers with the clockwise and counterclockwise dihedral angles. Remembering that the ratio of the $S_1 \rightarrow S_0$ hoppings via the clockwise S_1/S_0 conical intersection S1S0-1 and the counterclockwise S_1/S_0 conical intersection S1S0-2 is about 74% vs. 26%, one can deduce that 10% [31%] trajectories that hop to the S_0 state via the counterclockwise [clockwise] S_1/S_0 conical intersection S1S0-2 [S1S0-1] return to the S0-ZZ region; the remaining 43% and 16% trajectories go to the corresponding S0-ZE regions, respectively. Certainly, one should be noted that the above analysis is based merely on the final product distribution of 300 fs nonadiabatic dynamics simulation, which could only provide some qualitative insights.

To illustrate the clockwise and counterclockwise excited-state isomerization channels, we have plotted the time-dependent changes of the C2N3N4C5 and C2'N3'N4'C5' dihedral angles in two representative trajectories in which the cis-trans photoisomerization takes place to produce S0-ZE products, as shown in Figure S7. The left panel shows a trajectory that decays to the S_0 state at 53 fs via the clockwise photoisomerization channel, in which the reaction coordinates, i.e., the C2'N3'N4'C5' dihedral angle, increases from ca. 0° at the beginning, via ca. 90° at the hopping time, to ca. 180° at the end; while the C2N3N4C5 dihedral angle just oscillates slightly. On the other hand, in the right panel, the C2'N3'N4'C5' dihedral angle decreases from ca. 0° at the beginning, via ca. -90° at the hopping time, to ca. -180° at the end. Figure S8 shows two

representative trajectories in which the cis-trans photoisomerization is not completed and finally the S0-ZZ reactant is repopulated.

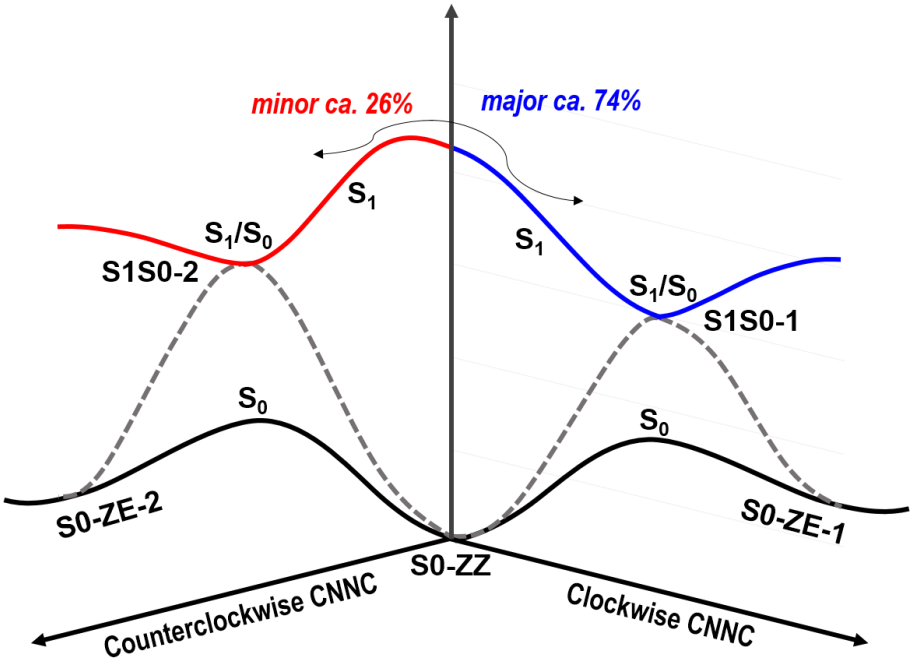

Figure 5. Suggested photoisomerization mechanism of the studied CBA molecule. See text for discussion.

Figure 5 summarizes the photoinduced isomerization and subsequent excited-state decay channels for the cis CBA molecule. Considering that both AB units in CBA are chemically equivalent, there are two different photoisomerization pathways with respect to the clockwise and counterclockwise rotation of the central N=N bond of each AB unit. However, the roles of these two pathways differ in the excited-state decay of CBA. In terms of our nonadiabatic dynamics simulations, it can be found that the clockwise photoisomerization via S1S0-1 is more favorable dynamically than its counterclockwise one via S1S0-2. The yield of trajectories via S1S0-1 versus S1S0-2 is estimated to be 74% vs. 26%. The preference of the excited-state decay channel via S1S0-1 is essentially from its barrierless photoisomerization path from the Franck-Condon point

to the S_1/S_0 minimum-energy conical intersection S1S0-1. Differing from S1S0-1, there is a subtle barrier for the excited-state decay path to S1S0-2, which is calculated to be 3.7 kcal/mol at the OM2/MRCI level. This small barrier leads to comparably distinct dynamical outcomes.

Our present OM2/MRCI calculations complement recent electronic structure calculations by Slavov et al. where the S_1 and S_0 potential energy surfaces, only relevant to the clockwise photoisomerization, are explored using the TD-DFT.[52] The topological structures of potential energy surfaces relevant to the cis-trans photoisomerization from the (Z,Z) to (Z,E) conformers are nearly the same as those calculated by us with the OM2/MRCI method. It is an almost barrierless process in both TD-DFT and OM2/MRCI levels for the clockwise pathway. Different from the clockwise situation, there is a small barrier of ca. 3.7 kcal/mol associated with the counterclockwise photoisomerization channel. Nevertheless, this excited-state decay pathway cannot be excluded because it contributes about 23% for the excited-state decay of CBA.

Previously combined experimental and theoretical work believe that the individual AB unit in CBA still undergoes the ultrafast Z-E photoisomerization in spite of the associated large steric hindrance and internal strain.[52] Our current nonadiabatic dynamics simulations support such viewpoint from dynamical perspective. In terms of our trajectories, the excited-state decay time is estimated to be ca. 69 fs, which is close previously reported values for isolated AB and its variants in different surroundings.

This kind of stereoselectivity for the excited-state decay has been previously found in isolated AB by Weingart et al., in which a ratio of ca. 77% vs. 23% is observed between the clockwise and counterclockwise photoisomerization pathways.[32] Later, one of the authors has found that in arylazopyrazole, a similar azo system, this stereoselectivity can be increased to ca. 97% vs. 3%.[96]

Motivated by this work, Pang and coworkers have recently this ratio can reach to ca. 99.7% vs. 0.3% in azoheteroarene systems.[101] All these path selectivity are caused by the fact that there are two different extent barriers associated with the clockwise and counterclockwise photoisomerization channels. Nevertheless, it should be stressed that to our best knowledge, this kind of stereoselectivity of excited-state decay is not reported for cyclic multiple AB systems. Our work demonstrates that this interesting phenomenon could be available in the complex cyclic system in which the AB units are linked by covalent bonds.

CONCLUSION

In summary, we have employed OM2/MRCI-based full-dimensional nonadiabatic dynamics simulation method to explore the S_1 photoisomerization mechanism and subsequent $S_1 \rightarrow S_0$ excited-state decay dynamics of a macrocyclic biazobenzene (CBA) molecule in which the two AB units are linked by covalent bonds. In terms of our electronic structure calculations, two relevant S_1/S_0 minimum-energy conical intersection structures are determined, which are responsible for the excited-state decay. Importantly, these two different conical intersections lead to two comparably important stereoselective photoisomerization and excited-state decay pathways, which separately correspond to the clockwise and counterclockwise photoisomerization motions with respect to the rotation of the N=N double bond of the central azo group. In both excited-state decay pathways, the excited-state isomerization and decay are found to be ultrafast and finished within ca. 69 fs, as estimated from on our dynamical trajectories. The most important finding is that our dynamics simulations reveal that the clockwise isomerization channel is much more favorable than the counterclockwise one with a ratio of 74% vs. 26%. Considering recent works, this ratio could be further enhanced to produce nearly exclusive stereoselective excited-state decay channel, which is very important for the realization of photoinduced molecular motors in which

the unidirectional motion is necessary. In one word, we have computationally demonstrated that stereoselective pathways not only exist in the photoisomerization of isolated azobenzene-like systems but also could be available in some macrocyclic systems with multiple AB units with strong steric hindrance and internal strain. This finding could pay the way for controlling the photodynamics of photoswitchable macrocyclic systems.

Supporting Information

Active orbitals in OM2/MRCI calculations, additional figures and tables, and Cartesian coordinates of all optimized structures.

Acknowledgments

This work is supported by National Natural Science Foundation of China (NSFC-21421003); G.C. is also grateful for financial supports from "Fundamental Research Funds for Central Universities". M. B. thanks the support of the Excellence Initiative of Aix-Marseille University (A*MIDEX) and the project Equip@Meso (ANR-10-EQPX-29-01), both funded by the French Government "Investissements d'Avenir" program.

References

(1) Beharry, A. A.; Woolley, G. A. Azobenzene Photoswitches for Biomolecules. *Chem. Soc. Rev.* **2011**, *40*, 4422–4437.

(2) Bandara, H. M. D.; Burdette, S. C. Photoisomerization in Different Classes of Azobenzene. *Chem. Soc. Rev.* **2012**, *41*, 1809–1825.

(3) Szymański,W.; Beierle, J. M.; Kistemaker, H. A. V.; Velema,W. A.; Feringa, B. L. Reversible Photocontrol of Biological Systems by the Incorporation of Molecular Photoswitches. *Chem. Rev.* **2013**, *113*, 6114–6178.

(4) Velema, W. A.; Szymanski, W.; Feringa, B. L. Photopharmacology: Beyond Proof of Principle. *J. Am. Chem. Soc.* **2014**, *136*, 2178–2191.

(5) Yurke, B.; Turberfield, A. J.; Mills Jr, A. P.; Simmel, F. C.; Neumann, J. L. A DNA-Fuelled Molecular Machine Made of DNA. *Nature* **2000**, *406*, 605–608.

(6) Norikane, Y.; Tamaoki, N. Light-Driven Molecular Hinge: A New Molecular Machine Showing a Light-Intensity-Dependent Photoresponse That Utilizes the trans-cis Isomerization of Azobenzene. *Org. Lett.* **2004**, *6*, 2595–2598.

(7) Henzl, J.; Mehhorn, M.; Morgenstern, K. Amino-Nitro-Azobenzene Dimers as a Prototype for a Molecular-Level Machine. *Nanotechnology* **2007**, *18*, 495502.

(8) Russew, M. M.; Hecht, S. Photoswitches: From Molecules to Materials. *Adv. Mater.* **2010**, *22*, 3348–3360.

(9) Bisoyi, H. K.; Li, Q. Light-Directing Chiral Liquid Crystal Nanostructures: From 1D to 3D. *Acc. Chem. Res.* **2014**, *47*, 3184–3195.

(10) Dong, M.; Babalhavaeji, A.; Samanta, S.; Beharry, A. A.; Woolley, G. A. Red-Shifting Azobenzene Photoswitches for in Vivo Use. *Acc. Chem. Res.* **2015**, *48*, 2662–2670.

(11) Kuzyk, A.; Yang, Y.; Duan, X.; Stoll, S.; Govorov, A. O.; Sugiyama, H.; Endo, M.; Liu, N. A Light-Driven Three-Dimensional Plasmonic Nanosystem That Translates Molecular Motion into Reversible Chiroptical Function. *Nat. Commun.* **2016**, *7*, 10591.

(12) Iwaso, K.; Takashima, Y.; Harada, A. Fast Response Dry-Type Artificial Molecular Muscles with [c2] Daisy Chains. *Nat. Chem.* **2016**, *8*, 626–633.

(13) Weis, P.; Wu, S. Light-Switchable Azobenzene-Containing Macromolecules: From UV to Near Infrared. *Macromol*. *Rapid Commun.* **2018**, *39*, 1700220.

(14) Zhao, T.; Wang, P.; Li, Q.; Al-Khalaf, A. A.; Hozzein, W. N.; Zhang, F.; Li, X.; Zhao, D. Near-Infrared Triggered Decomposition of Nanocapsules with High Tumor Accumulation and Stimuli Responsive Fast Elimination. *Angew. Chem. Int. Edit.* **2018**, *103*, 2611–2615.

(15) Rau, H.; Lueddecke, E. On the Rotation-Inversion Controversy on Photoisomerization of Azobenzenes. Experimental Proof of Inversion. *J. Am. Chem. Soc.* **1982**, *104*, 1616–1620.

(16) Nägele, T.; Hoche, R.; Zinth, W.; Wachtveitl, J. Femtosecond Photoisomerization of cis-Azobenzene. *Chem. Phys. Lett.* **1997**, *272*, 489–495.

(17) Rasmussen, P. H.; Ramanujam, P. S.; Hvilsted, S.; Berg, R. H. A Remarkably Efficient Azobenzene Peptide for Holographic Information Storage. *J. Am. Chem. Soc.* **1999**, *121*, 4738–4743.

(18) Fujino, T.; Arzhantsev, S. Y.; Tahara, T. Femtosecond Time-Resolved Fluorescence Study of Photoisomerization of trans-Azobenzene. *J. Phys. Chem. A* **2001**, *105*, 8123–8129.

(19) Ishikawa, T.; Noro, T.; Shoda, T. Theoretical Study on the Photoisomerization of Azobenzene. *J. Chem. Phys.* **2001**, *115*, 7503–7512.

(20) Schultz, T.; Quenneville, J.; Levine, B.; Toniolo, A.; Martínez, T. J.; Lochbrunner, S.; Schmitt, M.; Shaffer, J. P.; Zgierski, M. Z.; Stolow, A. Mechanism and Dynamics of Azobenzene Photoisomerization. *J. Am. Chem. Soc.* **2003**, *125*, 8098–8099.

(21) Chang, C.-W.; Lu, Y.-C.; Wang, T.-T.; Diau, E. W.-G. Photoisomerization Dynamics of Azobenzene in Solution with S_1 Excitation: A Femtosecond Fluorescence Anisotropy Study. *J. Am. Chem. Soc.* **2004**, *126*, 10109–10118.

(22) Cembran, A.; Bernardi, F.; Garavelli, M.; Gagliardi, L.; Orlandi, G. On the Mechanism of the cis-trans Isomerization in the Lowest Electronic States of Azobenzene: S_0, S_1, and T_1. *J. Am. Chem. Soc.* **2004**, *126*, 3234–3243.

(23) Ciminelli, C.; Granucci, G.; Persico, M. The Photoisomerization Mechanism of Azobenzene: A Semiclassical Simulation of Nonadiabatic Dynamics. *Chem. Eur. J.* **2004**, *10*, 2327–2341.

(24) Tiago, M. L.; Ismail-Beigi, S.; Louie, S. G. Photoisomerization of Azobenzene from First-Principles Constrained Density-Functional Calculations. *J. Chem. Phys.* **2005**, *122*, 094311.

(25) Toniolo, A.; Ciminelli, C.; Persico, M.; Martínez, T. J. Simulation of the Photodynamics of Azobenzene on Its First Excited State: Comparison of Full Multiple Spawning and Surface Hopping Treatments. *J. Chem. Phys.* **2005**, *123*, 234308.

(26) Crecca, C. R.; Roitberg, A. E. Theoretical Study of the Isomerization Mechanism of Azobenzene and Disubstituted Azobenzene Derivatives. *J. Phys. Chem. A* **2006**, *110*, 8188–8203.

(27) Renner, C.; Moroder, L. Azobenzene as Conformational Switch in Model Peptides. *ChemBioChem* **2006**, *7*, 868–878.

(28) Keiper, S.; Vyle, J. S. Reversible Photocontrol of Deoxyribozyme-Catalyzed RNA Cleavage under Multiple-Turnover Conditions. *Angew. Chem. Int. Edit.* **2006**, *118*, 3384–3387.

(29) Asanuma, H.; Liang, X.; Nishioka, H.; Matsunaga, D.; Liu, M.; Komiyama, M. Synthesis of Azobenzene-Tethered DNA for Reversible Photo-Regulation of DNA Functions: Hybridization and Transcription. *Nat. Protoc.* **2007**, *2*, 203.

(30) Conti, I.; Garavelli, M.; Orlandi, G. The Different Photoisomerization Efficiency of Azobenzene in the Lowest nπ* and ππ* Singlets: The Role of a Phantom State. *J. Am. Chem. Soc.* **2008**, *130*, 5216–5230.

(31) Ootani, Y.; Satoh, K.; Nakayama, A.; Noro, T.; Taketsugu, T. Ab initio Molecular Dynamics Simulation of Photoisomerization in Azobenzene in the nπ* state. *J. Phys. Chem. Lett.* **2009**, *131*, 194306.

(32) Weingart, O.; Lan, Z. G.; Koslowski, A.; Thiel, W. Chiral Pathways and Periodic Decay in cis-Azobenzene Photodynamics. *J. Phys. Chem. Lett.* **2011**, *2*, 1506–1509.

(33) Pederzoli, M.; Pittner, J.; Barbatti, M.; Lischka, H. Nonadiabatic Molecular Dynamics Study of the cis-trans Photoisomerization of Azobenzene Excited to the S_1 State. *J. Phys. Chem. A* **2011**, *115*, 11136–11143.

(34) Cusati, T.; Granucci, G.; Persico, M. Photodynamics and Time-Resolved Fluorescence of Azobenzene in Solution: A Mixed Quantum-Classical Simulation. *J. Am. Chem. Soc.* **2011**, *133*, 5109–5123.

(35) Gámez, J. A.; Weingart, O.; Koslowski, A.; Thiel, W. Cooperating Dinitrogen and Phenyl Rotations in trans-Azobenzene Photoisomerization. *J. Chem. Theory Comput.* **2012**, *8*, 2352–2358.

(36) Quick, M.; Dobryakov, A. L.; Gerecke, M.; Richter, C.; Berndt, F.; Ioffe, I. N.; Granovsky, A. A.; Mahrwald, R.; Ernsting, N. P.; Kovalenko, S. A. Photoisomerization Dynamics and Pathways of trans-and cis-Azobenzene in Solution from Broadband Femtosecond Spectroscopies and Calculations. *J. Phys. Chem. B* **2014**, *118*, 8756–8771.

(37) Yu, L.; Xu, C.; Zhu, C. Probing the π→π* Photoisomerization Mechanism of cis-Azobenzene by Multi-State ab initio on-the-fly Trajectory Dynamics Simulation. *Phys. Chem. Chem. Phys.* **2015**, *17*, 17646–17660.

(38) Goldau, T.; Murayama, K.; Brieke, C.; Steinwand, S.; Mondal, P.; Biswas, M.; Burghardt, I.; Wachtveitl, J.; Asanuma, H.; Heckel, A. Reversible Photoswitching of RNA Hybridization at Room Temperature with an Azobenzene C-Nucleoside. *Chem. Eur. J.* **2015**, *21*, 2845–2854.

(39) Tan, E. M.; Amirjalayer, S.; Smolarek, S.; Vdovin, A.; Zerbetto, F.; Buma, W. J. Fast Photodynamics of Azobenzene Probed by Scanning Excited-State Potential Energy Surfaces Using Slow Spectroscopy. *Nat. Commun.* **2015**, *6*, 5860.

(40) Xia, S.-H.; Cui, G. L.; Fang, W.-H.; Thiel, W. How Photoisomerization Drives Peptide Folding and Unfolding: Insights from QM/MM and MM Dynamics Simulations. *Angew. Chem. Int. Edit.* **2016**, *128*, 2107–2112.

(41) Titov, E.; Granucci, G.; Götze, J. P.; Persico, M.; Saalfrank, P. Dynamics of Azobenzene Dimer Photoisomerization: Electronic and Steric Effects. *J. Phys. Chem. Lett.* **2016**, *7*, 3591–3596.

(42) Fregoni, J.; Granucci, G.; Coccia, E.; Persico, M.; Corni, S. Manipulating Azobenzene Photoisomerization through Strong Light-Molecule Coupling. *Nat. Commun.* **2018**, *9*, 4688.

(43) Mondal, P.; Granucci, G.; Rastädter, D.; Persico, M.; Burghardt, I. Azobenzene as a Photoregulator Covalently Attached to RNA: A Quantum Mechanics/Molecular Mechanics-Surface Hopping Dynamics Study. *Chem. Sci.* **2018**, *9*, 4671–4681.

(44) Dokic, J.; Gothe, M.; Wirth, J.; Peters, M. V.; Schwarz, J.; Hecht, S.; Saalfrank, P. Quantum Chemical Investigation of Thermal Cis-to-Trans Isomerization of Azobenzene Derivatives: Substituent Effects, Solvent Effects, and Comparison to Experimental Data. *J. Phys. Chem. A* **2009**, *113*, 6763-6773.

(45) Bléger, D.; Dokic, J.; Peters, M. V.; Grubert, L.; Saalfrank, P.; Hecht, S. Electronic Decoupling Approach to Quantitative Photoswitching in Linear Multiazobenzene Architectures. *J. Phys. Chem. B* **2011**, *115*, 9930-9940.

(46) Floß, G.; Saalfrank, P. The Photoinduced E→Z Isomerization of Bisazobenzenes: A Surface Hopping Molecular Dynamics Study. *J. Phys. Chem. A* **2015**, *119*, 5026-5037.

(47) Slavov, C.; Yang, C.; Schweighauser, L.; Boumrifak, C.; Dreuw, A.; Wegner, H. A.; Wachtveitl, J. Connectivity Matters-Ultrafast Isomerization Dynamics of Bisazobenzene Photoswitches. *Phys. Chem. Chem. Phys* **2016**, *18*, 14795-14804.

(48) Shen, Y.-T.; Guan, L.; Zhu, X.-Y.; Zeng, Q.-D.; Wang, C. Submolecular Observation of Photosensitive Macrocycles and Their Isomerization Effects on Host-Guest Network. *J. Am. Chem. Soc.* **2009**, *131*, 6174–6180.

(49) Norikane, Y.; Hirai, Y.; Yoshida, M. Photoinduced Isothermal Phase Transitions of Liquid-Crystalline Macrocyclic Azobenzenes. *Chem. Commun.* **2011**, *47*, 1770–1772.

(50) Reuter, R.; Wegner, H. A. Switchable 3D Networks by Light Controlled π-Stacking of Azobenzene Macrocycles. *Chem. Commun.* **2013**, *49*, 146–148.

(51) Wagner-Wysiecka, E.; Łukasik, N.; Biernat, J. F.; Luboch, E. Azo Group(s) in Selected Macrocyclic Compounds. *J. Incl. Phenom. Macro.* **2018**, *90*, 189–257.

(52) Slavov, C.; Yang, C.; Heindl, A. H.; Stauch, T.; Wegner, H. A.; Dreuw, A.; Wachtveitl, J. Twist and Return-Induced Ring Strain Triggers Quick Relaxation of a (Z)-Stabilized Cyclobisazobenzene. *J. Phys. Chem. Lett.* **2018**, *9*, 4776–4781.

(53) Parr, R. G.; Yang, W. T. *Density-Functional Theory of Atoms and Molecules*; Oxford University Press, USA, 1994.

(54) Vosko, S. H.; Wilk, L.; Nusair, M. Accurate Spin-Dependent Electron Liquid Correlation Energies for Local Spin Density Calculations: A Critical Analysis. *Can. J. Phys.* **1980**, *58*, 1200–1211.

(55) Lee, C.; Yang, W. T.; Parr, R. G. Development of the Colle-Salvetti Correlation-Energy Formula into a Functional of the Electron Density. *Phys. Rev. B* **1988**, *37*, 785–789.

(56) Becke, A. D. Density-Functional Exchange-Energy Approximation with Correct Asymptotic Behavior. *Phys. Rev. A* **1988**, *38*, 3098–3100.

(57) Becke, A. D. A New Mixing of Hartree-Fock and Local Density-Functional Theories. *J. Chem. Phys.* **1993**, *98*, 1372–1377.

(58) Ditchfield, R.; Hehre, W. J.; Pople, J. A. Self-Consistent Molecular-Orbital Methods. IX. An Extended Gaussian-Type Basis for Molecular-Orbital Studies of Organic Molecules. *J. Chem. Phys.* **1971**, *54*, 724–728.

(59) Francl, M. M.; Pietro, W. J.; Hehre, W. J.; Binkley, J. S.; Gordon, M. S.; DeFrees, D. J.; Pople, J. A. Self-Consistent Molecular Orbital Methods. XXIII. A Polarization-Type Basis Set for Second-Row Elements. *J. Chem. Phys.* **1982**, *77*, 3654–3665.

(60) Frisch, M. J.; Trucks, G. W.; Schlegel, H. B.; Scuseria, G. E.; Robb, M. A.; Cheeseman, J. R.; Scalmani, G.; Barone, V.; Petersson, G. A.; Nakatsuji, H., Li, X.; Caricato, M.; Marenich, A. V.; Bloino, J.; Janesko, B. G.; Gomperts, R.; Mennucci, B.; Hratchian, H. P.; Ortiz, J. V.; Izmaylov, A. F.; Sonnenberg, J. L.; Williams-Young, D.; Ding, F.; Lipparini, F.; Egidi, F.; Goings, J.; Peng, B.; Petrone, A.; Henderson, T.; Ranasinghe, D.; Zakrzewski, V. G.; Gao, J.; Rega, N.; Zheng, G.; Liang, W.; Hada, M.; Ehara, M.; Toyota, K.; Fukuda, R.; Hasegawa, J.; Ishida, M.; Nakajima, T.; Honda, Y.; Kitao, O.; Nakai, H.; Vreven, T.; Throssell, K.; Montgomery, J. A., Jr.; Peralta, J. E.; Ogliaro, F.; Bearpark, M. J.; Heyd, J. J.; Brothers, E. N.; Kudin, K. N.; Staroverov, V. N.; Keith, T. A.; Kobayashi, R.; Normand, J.; Raghavachari, K.; Rendell, A. P.; Burant, J. C.; Iyengar, S. S.; Tomasi, J.; Cossi, M.; Millam, J. M.; Klene, M.; Adamo, C.; Cammi, R.; Ochterski, J. W.; Martin, R. L.; Morokuma, K.; Farkas, O.; Foresman, J. B.; Fox, D. J. *Gaussian 09*, Revision A.02. Gaussian, Inc., Wallingford CT, 2009.

(61) Marques, M. A. L.; Ullrich, C. A.; Nogueira, F.; Rubio, A.; Burke, K.; Gross, E. K. U. *Time-dependent Density Functional Theory*; Springer, 2006.

(62) Gámez, J. A.; Weingart, O.; Koslowski, A.; Thiel, W. Periodic Decay in the Photoisomerisation of p-Aminoazobenzene. *Phys. Chem. Chem. Phys.* **2013**, *15*, 11814–11821.

(63) Gámez, J. A.; Koslowski, A.; Thiel, W. Enhanced E→Z Photoisomerisation in 2-Aminoazobenzene. *RSC Adv.* **2014**, *4*, 1886–1889.

(64) Wu, D.; Wang, Y.-T.; Fang, W.-H.; Cui, G. L.; Thiel, W. QM/MM Studies on Photoisomerization Dynamics of Azobenzene Chromophore Tethered to a DNA Duplex: Local Unpaired Nucleobase Plays a Crucial Role. *Chem. Asian. J.* **2018**, *13*, 780–784.

(65) Weber, W. Ph.D. thesis, University of Zürich, 1996.

(66) Weber, W.; Thiel, W. Orthogonalization Corrections for Semiempirical Methods. *Theor. Chem. Acc.* **2000**, *103*, 495–506.

(67) Koslowski, A.; Beck, M. E.; Thiel, W. Implementation of a General Multireference Configuration Interaction Procedure with Analytic Gradients in a Semiempirical Context Using the Graphical Unitary Group Approach. *J. Comput. Chem.* **2003**, *24*, 714–726.

(68) Thiel, W. *MNDO99 program*, version 6.1.; Max-Planck-Institut für Kohlenforschung, Mülheim, Germany, 2007.

(69) Yarkony, D. R. Nuclear Dynamics near Conical Intersections in the Adiabatic Representation: I. The Effects of Local Topography on Interstate Transitions. *J. Chem. Phys.* **2001**, *114*, 2601–2613.

(70) Keal, T. W.; Koslowski, A.; Thiel, W. Comparison of Algorithms for Conical Intersection Optimisation Using Semiempirical Methods. *Theor. Chem. Acc.* **2007**, *118*, 837–844.

(71) Tully, J. C.; Preston, R. K. Trajectory Surface Hopping Approach to Nonadiabatic Molecular Collisions: Reaction of H with D2. *J. Chem. Phys.* **1971**, *55*, 562–572.

(72) Hammes-Schiffer, S.; Tully, J. C. Proton Transfer in Solution: Molecular Dynamics with Quantum Transitions. *J. Chem. Phys.* **1994**, *101*, 4657–4667.

(73) Fabiano, E.; Keal, T. W.; Thiel, W. Implementation of Surface Hopping Molecular Dynamics Using Semiempirical Methods. *Chem. Phys.* **2008**, *349*, 334–347.

(74) Virshup, A. M.; Punwong, C.; Pogorelov, T. V.; Lindquist, B. A.; Ko, C., Martinez, T. J. Photodynamics in Complex Environments: ab initio Multiple Spawning Quantum Mechanical/Molecular Mechanical Dynamics. *J. Phys. Chem. B*, **2008**, *113*, 3280-3291.

(75) Tao, H.; Levine, B. G.; Martínez, T. J. Ab Initio Multiple Spawning Dynamics Using Multi-State Second-Order Perturbation Theory. *J. Phys. Chem. A* **2009**, *113*, 13656–13662.

(76) Barbatti, M.; Aquino, A. J. A.; Szymczak, J. J.; Nachtigallová, D.; Hobza, P.; Lischka, H. Relaxation mechanisms of UV-photoexcited DNA and RNA nucleobases. *Proc. Natl. Acad. Sci.* **2010**, *107*, 21453–21458.

(77) Nachtigallová, D.; Zelený, T.; Ruckenbauer, M.; Müller, T.; Barbatti, M.; Hobza, P.; Lischka, H. Does Stacking Restrain the Photodynamics of Individual Nucleobases? *J. Am. Chem. Soc.* **2010**, *132*, 8261–8263.

(78) Cui, G. L.; Ai, Y.; Fang, W. Conical Intersection Is Responsible for the Fluorescence Disappearance Below 365 nm in Cyclopropanone. *J. Phys. Chem. A* **2010**, *114*, 730–734.

(79) Cui, G. L.; Fang, W. Ab Initio Based Surface-Hopping Dynamics Study on Ultrafast Internal Conversion in Cyclopropanone. *J. Phys. Chem. A* **2011**, *115*, 1547–1555.

(80) Cui, G. L.; Fang, W. Ab Initio Trajectory Surface-Hopping Study on Ultrafast Deactivation Process of Thiophene. *J. Phys. Chem. A* **2011**, *115*, 11544–11550.

(81) Richter, M.; Marquetand, P.; González-Vázquez, J.; Sola, I.; González, L. Femtosecond Intersystem Crossing in the DNA Nucleobase Cytosine. *J. Phys. Chem. Lett.* **2012**, 3, 3090–3095.

(82) Martínez-Fernández, L.; Corral, I.; Granucci, G.; Persico, M. Competing Ultrafast Intersystem Crossing and Internal Conversion: A Time Resolved Picture for the Deactivation of 6-Thioguanine. *Chem. Sci.* **2014**, *5*, 1336–1347.

(83) Cui, G. L.; Thiel, W. Generalized Trajectory Surface-Hopping Method for Internal Conversion and Intersystem Crossing. *J. Chem. Phys.* **2014**, *141*, 124101.

(84) Granucci, G.; Persico, M.; Zoccante, A. Including Quantum Decoherence in Surface Hopping. *J. Chem. Phys.* **2010**, *133*, 134111–134119.

(85) Spörkel, L.; Thiel, W. Adaptive Time Steps in Trajectory Surface Hopping Simulations. *J. Chem. Phys.* **2016**, *144*, 194108.

(86) Cui, G. L.; Lan, Z.; Thiel, W. Intramolecular Hydrogen Bonding Plays a Crucial Role in the Photophysics and Photochemistry of the GFP Chromophore. *J. Am. Chem. Soc.* **2012**, *134*, 1662–1672.

(87) Cui, G. L.; Thiel, W. Nonadiabatic Dynamics of a Truncated Indigo Model. *Phys. Chem. Chem. Phys.* **2012**, *14*, 12378–12384.

(88) Kazaryan, A.; Lan, Z. G.; Schäfer, L. V.; Thiel, W.; Filatov, M. Surface Hopping Excited-State Dynamics Study of the Photoisomerization of a Light-Driven Fluorene Molecular Rotary Motor. *J. Chem. Theory. Comput.* **2011**, *7*, 2189–2199.

(89) Schönborn, J. B.; Koslowski, A.; Thiel, W.; Hartke, B. Photochemical dynamics of E-iPr-furylfulgide. *Phys. Chem. Chem. Phys.* **2012**, *14*, 12193–12201.

(90) Cui, G. L.; Thiel, W. Photoinduced Ultrafast Wolff Rearrangement: A Non-Adiabatic Dynamics Perspective. *Angew. Chem. Int. Ed.* **2013**, *52*, 433–436.

(91) Spöerkel, L.; Cui, G. L.; Thiel, W. Photodynamics of Schiff Base Salicylideneaniline: Trajectory Surface-Hopping Simulations. *J. Phys. Chem. A* **2013**, *117*, 4574–4583.

(92) Spöerkel, L.; Cui, G. L.; Koslowski, A.; Thiel, W. Nonequilibrium H/D Isotope Effects from Trajectory-Based Nonadiabatic Dynamics. *J. Phys. Chem. A* **2014**, *118*, 152–157.

(93) Schönborn, J. B.; Hartke, B. Photochemical Dynamics of E-methylfurylfulgide-Kinematic Effects on Photorelaxation Dynamics of Furylfulgides. *Phys. Chem. Chem. Phys.* **2014**, *16*, 2483–2490.

(94) Shemesh, D.; Blair, S. L.; Nizkorodov, S. A.; Gerber, R. B. Photochemistry of Aldehyde Clusters: Cross-Molecular versus Unimolecular Reaction Dynamics. *Phys. Chem. Chem. Phys.* **2014**, *16*, 23861–23868.

(95) Xia, S.-H.; Xie, B.-B.; Fang, Q.; Cui, G. L.; Thiel, W. Excited-State Intramolecular Proton Transfer to Carbon Atoms: Nonadiabatic Surface-Hopping Dynamics Simulations. *Phys. Chem. Chem. Phys.* **2015**, *17*, 9687–9697.

(96) Wang, Y.-T.; Liu, X.-Y.; Cui, G. L.; Fang, W.-H.; Thiel, W. Photoisomerization of Arylazopyrazole Photoswitches: Stereospecific Excited-State Relaxation. *Angew. Chem. Int. Edit.* **2016**, *55*, 14009–14013.

(97) Garcia-Iriepa, C.; Marazzi, M.; Zapata, F.; Valentini, A.; Sampedro, D.; Frutos, L. M. Chiral Hydrogen Bond Environment Providing Unidirectional Rotation in Photoactive Molecular Motors. *J. Phys. Chem. Lett.* **2013**, *4*, 1389-96.

(98) Marchand, G.; Eng, J.; Schapiro, I.; Valentini, A.; Frutos, L. M.; Pieri, E.; Olivucci, M.; Leonard, J.; Gindensperger, E. Directionality of Double-Bond Photoisomerization Dynamics Induced by a Single Stereogenic Center. *J. Phys. Chem. Lett.* **2015**, *6*, 599-604.

(99) Strambi, A.; Durbeej, B.; Ferre, N.; Olivucci, M. Anabaena Sensory Rhodopsin Is a Light-Driven Unidirectional Rotor. *Proc. Natl. Acad. Sci. U.S.A* **2010**, *107*, 21322-6.

(100) Wang, J.; Oruganti, B.; Durbeej, B. Light-Driven Rotary Molecular Motors without Point Chirality: A Minimal Design. *Phys. Chem. Chem. Phys.* **2017**, *19*, 6952-6956.

(101) Pang, X.; Jiang, C.; Qi, Y.; Yuan, L.; Hu, D.; Zhang, X.; Zhao, D.; Wang, D.; Lan, Z.; Li, F. Ultrafast Unidirectional Chiral Rotation in the Z-E Photoisomerization of Two Azoheteroarene Photoswitches. *Phys. Chem. Chem. Phys.* **2018**, *20*, 25910–25917.

TOC Graphic

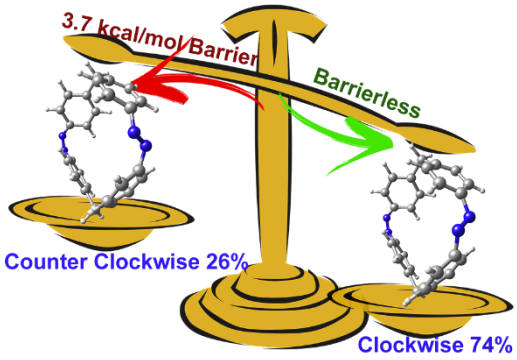
3.7 kcal/mol Barrier
Barrierless
Counter Clockwise 26%
Clockwise 74%